Package for the Interactive Analysis of Line Emission: Markov-Chain and Monte Carlo Methods

LiWei Lin, Vinay L. Kashyap, Jeremy J. Drake

Smithsonian Astrophysical Observatory

60 Garden St., Cambridge, MA 02138

pintofale@head.cfa.harvard.edu

Abstract

We describe the implementation of Monte Carlo methods in the Package for Interactive Analysis of Line Emission (PINTofALE), which is a collection of IDL-based programs designed to analyze astrophysical spectra. We use Monte Carlo based methods to determine errors in spectral line parameters, and use Markov-Chain Monte Carlo methods to construct emission measure distributions which summarize the structure of the coronae of stars. We present examples of how the algorithms are used and discuss some planned updates.

1. Introduction

The Package for Interactive Analysis of Line Emission (PINTofALE; Kashyap & Drake [17]) was developed for the analysis of line emission from stellar coronal plasma.[1] Most normal stars have hot atmospheres at temperatures of 1-10 MK that emit optically thin thermal radiation in the extreme-UV and X-ray wavelength range. The spectra are dominated by line emission from highly ionized species of abundant Fe, O, Ne, etc., as well as continuum emission from free-free (Bremsstrahlung) and free-bound radiation. Analysis of such spectra requires access to the innards of atomic line databases as well as flexible tools for interactive modeling. PINTofALE is a collection of modular routines written in IDL[2]. IDL is a versatile scripting language used extensively by astrophysicists, and provides for the development of both command-line driven and GUI based applications. The PINTofALE routines provide easy access to pre-compiled atomic databases and perform basic spectral analysis tasks such as line identification, profile fitting, and the creation of synthetic spectra.

Here we present several implementations of Monte Carlo methods in PINTofALE. The most sophisticated of these is a Markov-Chain Monte Carlo (MCMC) analysis package geared towards the problem of reconstructing Differential Emission Measures (DEMs). DEMs describe the "amount of material" contributing to coronal emission at a given temperature, and are thus a key probe of coronal structure. DEM reconstruction via MCMC allows confidence bound estimation, automatic de-blending of lines, use of robust data such as line ratios, and avoids non-physical smoothness constraints which other methods are prone to. We demonstrate these capabilities by performing DEM reconstruction on a synthetic *Chandra*/HETG spectrum generated using a known DEM. Monte Carlo and MCMC methods have attained increasing popularity in a diverse range of scientific endeavor in both industrial and academic applications. Their acclaim is well-deserved, as they, together with exponentially growing and affordable computational power, provide a means for efficient sampling of complicated high dimensional parameter spaces, allowing scientists to probe data with increasingly sophisticated models, and tackle problems previously considered intractable. Here we begin by giving a cursory overview of some basic concepts in coronal plasma physics in §2. This will serve both to illuminate the context in which analysis software such as PINTofALE is necessary, as well as provide a platform from which we can discuss the problem of DEM reconstruction. In §3, we describe the general structure of PINTofALE. Then in §4, we describe the implementation of some Monte Carlo based techniques in PINTofALE, and summarize the application of these implementations in §5.

2. Coronal Plasma and Emission Measure Analysis

Most normal stars, including the Sun, have hot outer atmospheres where temperatures range from 10^5 K to $>$

---

1 See `http://hea-www.harvard.edu/PINTofALE/`, where PINTofALE is described in detail, and from where the software can be freely downloaded.

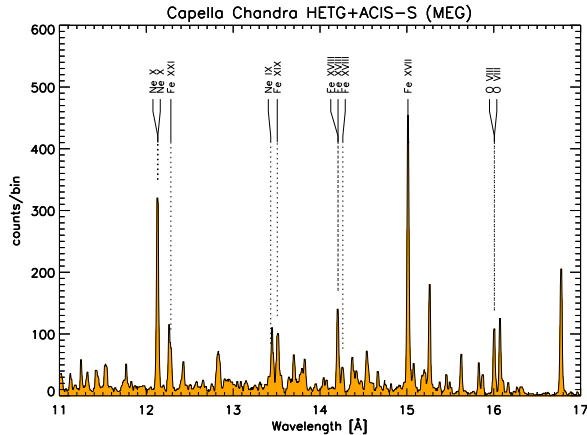2 Interactive Data Language[TM], developed by Research Systems Inc., of Boulder, CO.

Figure 1. A high resolution (*Chandra*) spectrum of Capella. The co-added MEG spectrum from an ACIS-S/HETG observation is shown as the shaded gray region from 11 to 17 angstroms. The dashed lines point to the locations of some astrophysically important lines. These are labeled with the ionic species responsible for the transition.

10^7 K and the density is typically $10^9 - 10^{12}$ cm^{-3}. Such conditions give rise to highly ionized elements, and collisionally dominated optically thin emission which peaks in the X-ray range. At temperatures above $\sim 10^6$ K the spectrum is dominated by emission from H-like and He-like species of the most abundant elements (O, Si, Mg, Ne, Ar, S, Fe, N, and C), and by continuum energy losses. The high spectral resolution available on the current generation of X-Ray satellites (e.g. *Chandra*, and *XMM-Newton*) brings numerous plasma diagnostics within reach that were unavailable with low-spectral-resolution data from previous missions such as *Einstein*, *ROSAT*, *ASCA*, etc. As an illustration of the rich spectral data available, we show a *Chandra*/HETG spectrum of the active spectroscopic binary Capella (α Aur) in Figure 1, where some of the stronger H-like and He-like emission lines are identified and labeled.

An individual emission line is characterized by its identification (i.e., the ionic species from which it originates, and the quantum levels that define the transition itself), the energy of the transition (the wavelength, usually in Å), the intensity (usually in counts per bin or flux in photons cm^{-2} s^{-1}), and the shape of the profile (which is a combination of intrinsic shape, thermal and Doppler broadening, and instrumental broadening). Of particular interest is the integrated flux of these lines or what the ratios of the fluxes of some interesting lines can tell us about the physical properties of the coronal plasma under scrutiny - temperature structure, electron density, and relative abundances of elements.

A formalism to address such questions was first developed by Pottasch [21] for UV analysis of the solar corona, and later by Jefferies e.g. Orral & Zirker [12], Withbroe [26], Jordan [13] and Craig & Brown [6]. For a transition $u \to l$ the intensity is given by

$$I_{ul} = AK_{ul} \int_T G_{ul}(n_e, T) n_e^2 dV(T) \qquad (1)$$

where A is the elemental abundance relative to H, $G_{ul}(n_e, T)$ are the atomic emissivities or line cooling functions which represent the response of the intensity of a given transition at a given temperature T and electron density n_e, K_{ul} is a constant factor that takes into account the energy of the transition and the distance to the source, $n_e^2 dV(T)$ is the *Emission Measure*, which indicates the amount of material existing at a given temperature, and $dV(T)$ is the volume occupied by the plasma at temperature T. Compilations of atomic data are available from databases such as CHIANTI (Dere et al. [7]), SPEX (Kaastra et al. [15]), and APED (Brickhouse et al. [3], Smith et al. [25]).

If we ignore the slight density sensitivity in the line cooling function and integrate over T rather than volume, we can recast the equation as:

$$I_{ul} = AK_{ul} \int_T G_{ul}(T) n_e^2 \frac{dV(T)}{dT} dT \qquad (2)$$

where we define the Differential Emission Measure:

$$DEM(T) = n_e^2 \frac{dV(T)}{dT} . \qquad (3)$$

With the availability of high resolution spectra from *Chandra* and *XMM-Newton*, much effort has been geared towards the development of DEM reconstruction methods. Given line fluxes observed for N different lines for which $G_{ul}(n_e, T)$ can be calculated, and given adequate temperature coverage by these line cooling functions, one obtains a system of N integral equations for which the DEM is an unknown kernel and the abundances must be derived. This is an instance of Fredholm's equation of the first type, and straightforward inversion poses well-known mathematical difficulties. For instance, the solution is non-unique and is subject to high-frequency instability. We avoid these issues by forward fitting, i.e., deriving a best-fit solution with errors, and imposing physics-based smoothness constraints.

The DEM reconstruction problem has been addressed by several authors using Singular Value Decomposition (Schmitt et al. [24]), spline curve fitting (Brosius et al. [4]), and fitting with Chebychev polynomials (Schmitt & Ness [23]), amongst others (Kaastra et al. [15]); see Judge, Hubeny, & Brown [14] for a critique of the process.

We present here a DEM reconstruction algorithm based on a Markov-Chain Monte Carlo reconstruction method developed by Kashyap & Drake [16]. We demonstrate this method below (see §4.3) on a synthetic *Chandra*/HETG spectrum generated with PINTofALE routines.

3. Package for Interactive Analysis of Line Emission: Creation of Synthetic spectra

PINTofALE is a software suite of modularized IDL routines geared towards, but not limited to, the analysis of coronal plasma line emission. The mission of the project is to fuse the otherwise disparate and various atomic database and data analysis packages necessary for high energy spectral analysis into one transparent, flexible, and freely available software package. The collection of PINTofALE routines can be roughly grouped by function as follows:

- **Atomic Database Compilation and Data Mining:** PINTofALE's atomic data base compilation routines interact with atomic line databases (external to PINTofALE), to compute and compile wavelengths and emissivities for available transitions that are then stored in a virtual catalog for quick retrieval. Data Mining routines retrieve the pre-compiled data flexibly and on demand. Currently supported atomic line databases include CHIANTI, APED, and SPEX.

- **Analysis:** Core analysis routines allow the user to interactively analyze emission line spectra via both GUI-based and command line based routines. They perform the basic analysis tasks required. For instance, `PICKRANGE()` allows 'spectral browsing', or dynamic mouse-controlled changing of wavelength regimes on an intensity v/s wavelength plot; `LINEID()` is a GUI-based line identification program; `FITLINES()` allows GUI-based interactive model fitting of individual or multiple emission features with Gaussian, Lorentzian, or other functions; `MIXIE()` is a command-line–based routine which can identify possible blends of interesting lines and return correction factors for their measured fluxes, etc. Other routines in this category perform tasks such as Levenberg-Marquardt least square minimization, calculation of interstellar absorption, and convolution of model spectra with instrumental line response function.

- **Utilities:** PINTofALE's utilities are designed to aid in miscellaneous functionality that are not specific to spectral analysis but are likely to be of interest to a general user. Examples of this include a compilation of fundamental constants (`INICON`), histogram generation (`HASTOGRAM()`), re-binning into an arbitrary binning while conserving flux (`REBINW()`), placing labels on plots (`PLOTID`), fitting functions to data (`FIT_LEVMAR`), etc.

The steps necessary to create a simulated spectrum with PINTofALE are as follows:

1. INITALE: Initialize the stellar coronal parameters electron density n_e, abundances $A(Z)$, and absorption column density N_H.

2. MK_DEM() : Set the initial Differential Emission Measure

3. RD_LINE() and RD_CONT() : load the atomic line and continuum emissivities

4. FOLD_IONEQ() : fold ion balance calculations into line emissivity functions

5. LINEFLX(): compute continuum and line fluxes by integrating the emissivities, weighted by the DEM, over temperature.

6. ISMTAU(): correct for interstellar absorption

7. RDARF() : read in the instrument effective area

8. HASTOGRAM() : bin the line and continuum fluxes

9. add line and continuum spectra, weighted by effective area

10. CONV_RMF : Convolve the predicted flux spectrum with instrumental response matrix and multiply by exposure time to get a predicted counts spectrum.

Though one may argue that preparing the different modules can be a time consuming project, one must note that this modularization makes PINTofALE highly flexible and offers the user true hands on control of the analysis, rather than produce a 'black box' package that will invariably be misused because of its complexity. Nevertheless, for such common tasks as creation of a synthetic spectrum that may require the orchestration of an array of PINTofALE routines in a repeatable and well-understood manner, PINTofALE also includes the option of using pre-packaged scripts which run the routines in a batch to perform a required task. The script `XMMS_epic_rgs_ao3.par` is an example: it allows the user to create a synthetic *XMM*/RGS spectrum by simply toggling the relevant parameters in the script header.

4. Monte Carlo methods in PINTofALE

4.1. Monte Carlo Error Estimation

Error estimation via Monte Carlo is an efficient tool with which we determine the confidence bounds on model parameters in those cases where the fits involve prohibitively large numbers of parameters. Propagating errors for large parameter sets and handling it analytically or even numerically, especially when considering strong correlations that
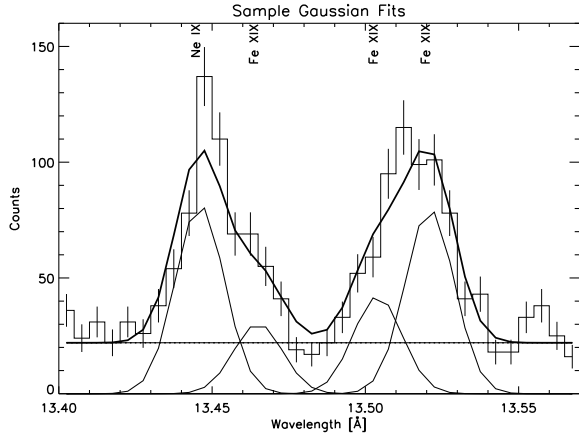
Figure 2. Sample fits of the heavily blended Ne IX region. Plotted over the spectrum (stepped histogram with error bars shown as vertical bars) are the continuum level (horizontal line), four Gaussian profiles for each line, and a composite of the five components. The fits were made using PINTofALE 's GUI-based line fitting software. Error analysis of such fits requires attention to strong correlations between the modeled integrated fluxes of the individual lines.

may exist between parameters (when covariance terms become important), may require an expert's knowledge of an array of statistical techniques that apply differently to different cases.

To illustrate, we use a simple example pertinent to our discussion of emission line spectroscopy. In Figure 2, we show a region of the *Chandra*/HETG spectrum of Capella (Figure 1) where we have identified a strong resonance line from Ne IX and 3 contaminant lines originating from Fe XIX. A Gaussian profile is assigned to each of the four lines, each having 3 parameters: width, position, and flux. Together with a continuum level, they give a composite curve with which to fit the observed counts spectrum in this wavelength region. The Ne IX resonance line is part of a temperature-sensitive diagnostic, and measuring its flux accurately is generally of prime importance. Even after applying all known constraints, e.g., the widths of all the lines may be approximated by the instrument width, and line positions are quite well determined by referring to the atomic database, this situation presents a challenge to classical model fitting methods. Further, if we are to require reliable errors on the fit parameters, we must also account for the fact that because the profiles are so heavily blended with each other, their fluxes are strongly correlated. Thus, rather

than proceeding with the task analytically, we take a Monte Carlo approach. Adhering to a method described in detail by Press et al. [22], we:

1. create N synthetic data sets by varying the true data set randomly within its observed error

2. fit the N synthetic data sets in the same way that the original data set was analyzed, achieving N fitted sets of fluxes

3. characterize the uncertainty in our original fit by observing how the N sets of fluxes achieved synthetically are distributed about the original parameters. We may do this, e.g., by delineating confidence bounds with a χ^2 statistic, or by measuring a confidence width in parameter space by counting simulated parameters starting from the true fit out towards a required confidence (e.g. 68% or 90%).

We have incorporated this method of error analysis in PINTofALE's GUI based line fitting software. Preliminary tests of the method on single line fits (non-correlated parameters) give results which are largely in agreement with standard error computation methods.

4.2. Model Optimization with Markov Chain Monte Carlo

In general terms, the task of the astrophysicist often is to optimize a parameterized model to an observed data set to infer physically meaningful quantities with maximum confidence given the quality of the data. Given say, m data points $D = \{D_i, i = 1...m\}$ each with its associated error, and a proposed model with N parameters, $\Theta = \{\theta_\nu, \nu = 1...N\}$, the task is to find that Θ which best models the data according to some specified merit function. Put another way, we seek to maximize the probability of observing parameters D given a model Θ, by assessing for example $P(D|\Theta) = exp(-1/2 \sum_{i=1}^{m}((D_{i_{obs}} - D_{i_{mod}})/\sigma_{i_{obs}})^2)$ for different sets of Θ, with $D_{i_{mod}}$ being the data set calculated using the model evaluated for Θ, to compare with an observed data set $D_{i_{obs}}$ with associated error $\sigma_{i_{obs}}$.

It is often the case that one may proceed fruitfully by employing standard methods such as Levenberg-Marquardt minimization, which calculates gradients in parameter space to use as a guide in an iterative stepping process towards areas of high likelihood, after which a solution to the N dimensional problem is approximated. Such a process can however become ill-suited if one encounters a problem with a relatively large number of parameters characterizing the model for a middling number of data points.

In an ideal world, where computational power is no object, one can envision that such complex parameterized

problems can be solved by a brute force Monte Carlo process. A copious amount of sets Θ can be randomly generated and could sample a merit function in N dimensional parameter space with resolution adequate to not only give a good estimate of the best probability set Θ but also the projected confidence or credible bounds in the ascertained parameters. Realistically, a Monte Carlo approach would require some sort of conditioning mechanism to make those few simulations which are computationally tractable to actually count. A Markov Chain is exactly such a mechanism. A Markov chain is an ordered sequence of random variables (in our case parameter sets), $\Theta_0, \Theta_1, \Theta2, ...,$ in which the likelihood that a certain set Θ_{i+1} appear in the sequence is directly dependent only on Θ_i. Put in terms of conditional probabilities: $P(\Theta_{j+1}|\Theta_j, ...\Theta_0) = P(\Theta_{j+1}|\Theta_i)$. A set of transition rules can be adopted to govern the evolution of variables within such a sequence, For example, we adopt two such transition rules: First, the candidates for the next parameter set $\Theta^\star$ in sequence are obtained as Normal deviates of the current parameter set Θ: $\theta^\star = \theta + r\sigma$ where r is a random number and σ is an estimate of the variance of θ; and second, the Metropolis criterion [19], where candidate parameter sets are adopted with a probability $A(\Theta, \Theta^\star) = min[1, \frac{P(D|\Theta^\star)}{P(D|\Theta)}]$, i.e. a new parameter set is sometimes adopted even if its associated probability is smaller than that of the previously adopted set, a tactic designed to avoid having the solution get bogged down in local minima.

The discerning nature of the Markov Chain coupled with the randomized search of the Monte Carlo provides a computationally feasible method to harness the power of Monte Carlo. The 'random walk' nature of the MCMC approach allows the algorithm to probe regions of parameter space which might otherwise be ignored (e.g., χ^2 minimization routines often follow the steepest gradients in parameter space, not necessarily the gradient leading to the deepest valley). Moreover, simulations are run in batches, assuring adequate sampling of local parameter space, and would make apparent any non-uniqueness in the parameter solution. For a review of MCMC methods see Neal [20].

A generalized fitting engine employing MCMC is in the process of being built and incorporated into PINTofALE. In the following, we describe one instance of such an algorithm, one developed specifically to address the issue of stellar coronal DEMs (see §2).

4.3. Markov-Chain Monte Carlo DEM Reconstruction

In the language used to describe MCMC above, the DEM reconstruction problem is to maximize the probability of a modeled DEM and abundances given a set of measured line or continuum fluxes or flux ratios. That is, the task is to assess a merit function $P(D|\Theta) = exp(-1/2 \sum_{i=1}^{m}((I_{i_{obs}} - I_{i_{mod}})/\sigma_{i_{obs}})^2)$ where Θ is a parameter set used to model the DEM, $I_{i_{obs}}$ are measured fluxes with associated error $\sigma_{i_{obs}}$, and $I_{i_{mod}}$ are model fluxes calculated with Eq 1 using a DEM model evaluated for Θ and using emissivity curves from an atomic database. [3] Note that the exponent is just the well known expression for χ^2.

There are several approaches to how one can parameterize the DEM. These can be grouped into two general categories: continuous models which parameterize using a few control parameters (e.g. splines or Chebychev polynomials) and discrete models, where the DEM is an array of N temperature bins, giving essentially N model parameters (e.g. Singular Value Decomposition, the Regularization Method, genetic algorithms). Continuous models truncate the number of free parameters, thereby making the problem tractable for common minimization techniques (e.g. Levenberg-Marquardt). Their major drawback however is that assuming a functional form can impose non-physical constraints on the shape of the DEM. Also, probing a parameter space with standard χ^2 minimization techniques is prone to find local minima and will sometimes incur parameter degeneracy and non-unique solutions. The major advantage of a discretized parameterization is that it can approximate both continuous and discontinuous functional forms for the DEM. Its ability to do so however, depends on how fine one is willing to define the binning scheme and what constraints one places on the smoothness of the final solution. One can imagine for example, a DEM defined between $Log(T) = 5.5$ and $Log(T) = 7.8$ discretized with modest 0.1 dex bins will give 23 free parameters. Such a parameterization is intractable with e.g., Levenberg-Marquardt, as the number of data points available is generally limited to the $\simeq 10$ strong emission lines and/or flux ratios available in the spectra.

Kashyap & Drake [16] offer the latter approach to DEM reconstruction problem using a Markov-Chain Monte Carlo process. Their approach is now made available via the PINTofALE procedure MCMC_DEM. The procedure is highly flexible, offering the user a range of inputs allowing users to control the number of simulations, specify line ratios, allow different types of smoothing, censor data points (i.e., use upper and lower limits), etc. The output of the simulations are stored and are an ideal resource to characterize the uncertainty in the reconstructions.

It is important to realize that the MCMC algorithm implemented here cannot be used as a black box. While highly flexible and capable of addressing almost any type of as-

---

3   It is possible to use other statistics, such as Cash or Castor [5] to determine the likelihoods in the Poisson regime. However, the $e^{-\frac{1}{2}\chi^2}$ statistic used here by default is the best choice for DEM analysis, since the fluxes input for analysis are usually in intensity units (not photon counts) and are also background subtracted.
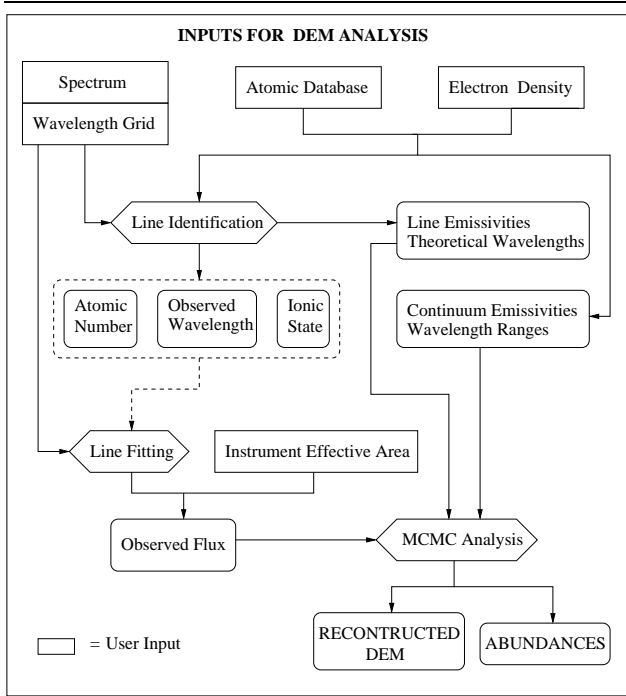
INPUTS FOR DEM ANALYSIS

Figure 3. Data flow chart of input parameters required for MCMC_DEM(). The direction of the arrows correspond to the direction of the data flow. Square rectangles indicate user inputs. Hexagons indicate analysis using PINTofALE software. Rounded rectangles indicate substantial analysis operations which have been generally encoded as stand-alone routines in PINTofALE . Rounded rectangles indicate analysis products.
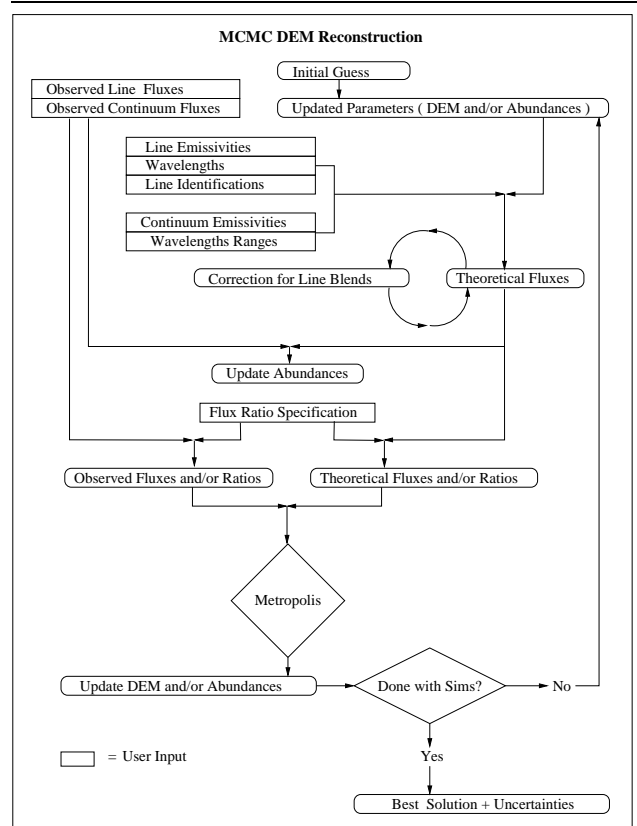

MCMC DEM Reconstruction

Figure 4. Data flow chart depicting the DEM realization process within MCMC_DEM(). The direction of the arrows indicate the direction of the data flow. Square rectangles indicate user inputs. Rounded rectangles indicate a computational result. Diamonds indicate a logic gate.

5. Application and Summary

We have tested the PINTofALE procedure MCMC_DEM exhaustively, both on synthetic spectra as well as actual high-resolution spectral data. One such test is shown as an example here. We first compute a synthetic spectrum (assuming Gaussian errors of 10 %) after adopting an arbitrary DEM with a double Lorentzian structure (maxima at $10^{6.6}$ K and $10^{7}.1$ K; see Figure 5). The spectrum is generated assuming solar abundance values (Grevesse & Sauval [11]). From this spectrum, a set of lines from H-like and He-like species were identified (using LINEID()). Lines from some of the most abundant species, O, Ne, Mg, Si, and S were chosen because they are relatively strong and their atomic data are the most reliable and well understood. Using PINTofALE, we identified a set of 24 of these lines

tronomical dataset, it does require of the user a measure of understanding of the process. This is the first algorithm of its kind made generally available to the astronomical community: there is no other DEM reconstruction method that computes uncertainties as a matter of course, nor one so general, and no MCMC based reconstruction algorithm. The complexity of the algorithm can be seen in the data flow diagram setting up the *input* to MCMC_DEM (Figure 3) and the data flow diagram of the MCMC DEM reconstruction algorithm itself (Figure 4). This process is of course also subject to yet more systematic uncertainties that arise from an imperfect knowledge of the underlying atomic data and the approximations made to the physics of the source (see Judge et al. [14], Kashyap & Drake [16]).
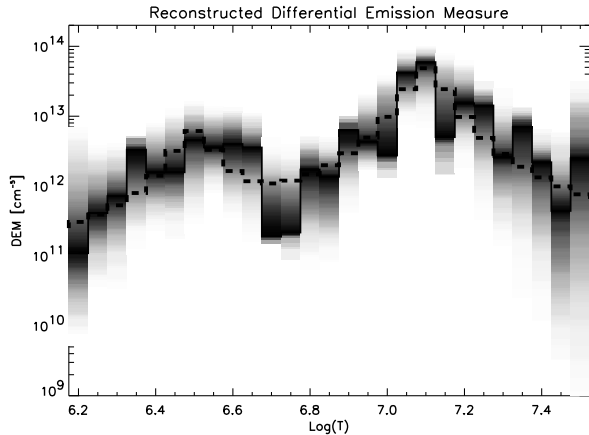
Reconstructed Differential Emission Measure

Figure 5. The reconstructed DEM distribution compared with the original. The original is plotted with a thick, dashed black line. In the top panel, the uncertainty in the DEM is displayed by plotting simulated emission measures within one sigma of the best value for each bin.
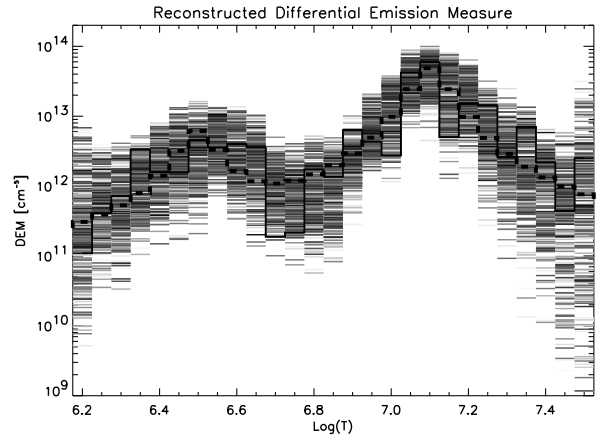

Reconstructed Differential Emission Measure

Figure 6. The reconstructed DEM distribution compared with the original. The uncertainty in the DEM is displayed by plotting all DEM realizations with the shade of grey indicating the probability associated with each. Darker shades indicate a better probability.

and measured line fluxes by fitting Gaussian profiles (`FIT-LINES()`) and correcting for the instrument effective area. We then set up the MCMC analysis (see Figure 3) by reading in the appropriate emissivities.

We ran an abundance invariant DEM reconstruction analysis using H-like/He-like ratios of lines from common elements (e.g. O VII/O VII, Ne IX/Ne X, Fe VIII/Fe VII etc.)(Drake et. al. [9]. A smoothing scale derived internally based on the widths of the emissivity functions was used to damp out the high-frequency oscillations inherent in this type of integrals (Equation 2; this is a Fredholm integral of the 1st kind). In a preliminary analysis, we run 500 simulations, which required around 7 minutes with an AMD Athlon 1800 Mhz processor.

The result of the reconstruction are shown as the shaded band in Figure 5, where the width of the band tracks the uncertainty in the DEM. All the simulated DEMs within the 1-σ level are shown. We can also characterize the uncertainty by plotting the 50% most probable DEMs (Figure 6). Both Figure 5 and Figure 6 were made with `MCMC_PLOT` an accessory routine to `MCMC_DEM`).

This MCMC based DEM reconstruction technique has also been applied to the analysis of many X-ray active stars: Drake et al. [8] have applied it to ξ Boo A, Maggio et al. [18] to solar analogs AD Leo and π^1 UMa, Argiroffi et al. [1] to Capella (α Tau), Ball et al. [2] to ξ UMa, and Garcia et al. [10] to AB Dor and V471 Tau, all using beta versions of

PINTofALE MCMC software.[4]

In summary, we have made a major upgrade to the PINTofALE suite of routines designed to facilitate the analysis of high-resolution spectral data. These will be made publicly available as PINTofALE v2 on April 7, 2004. The most significant improvements have been the addition of Monte Carlo based methods, all of which are aimed at providing better error bars for complex fitting problems, including the classically intractable problem of placing confidence bounds on reconstructed DEMs.

References

[1] C. Argiroffi, A. Maggio, and G. Peres. On coronal structures and their variability in active stars: The case of Capella observed with Chandra/LETGS. *Astronomy & Astrophysics*, 404:1033–1049, June 2003.

[2] W. Ball, J. Drake, L. Lin, and V. Kashyap. Stellar Coronal Abundnaces at Intermediate Activity Levels:ξ UMa. To be submitted to the *Astrophysical Journal* .

---

4 A guide to using `MCMC_DEM` is available online at `http://hea-www.harvard.edu/PINTofALE/doc/MCMC_DEM. html`.

[3] N. S. Brickhouse, R. K. Smith, and J. C. Houck. Spectroscopic Data for Modeling Highly Ionized Astrophysical Plasmas. *Bulletin of the American Astronomical Society*, 31:736–+, Apr. 1999.

[4] J. W. Brosius, J. M. Davila, R. J. Thomas, and B. C. Monsignori-Fossi. Measuring Active and Quiet-Sun Coronal Plasma Properties with Extreme-Ultraviolet Spectra from SERTS. *Astrophysical Journal Supplement*, 106:143–+, Sept. 1996.

[5] W. Cash. Parameter estimation in astronomy through application of the likelihood ratio. *Astrophysical Journal*, 228:939–947, Mar. 1979.

[6] I. J. D. Craig and J. C. Brown. Fundamental limitations of X-ray spectra as diagnostics of plasma temperature structure. *Astronomy & Astrophysics*, 49:239–250, June 1976.

[7] K. P. Dere, E. Landi, H. E. Mason, B. C. Monsignori Fossi, and P. R. Young. CHIANTI - an atomic database for emission lines. *A&A Supplement Series*, 125:149–173, Oct. 1997.

[8] J. J. Drake and V. Kashyap. The Coronal Metallicity of the Intermediate Activity Dwarf ξ Bootis A. *Astrophysical Journal*, 547:428–436, Jan. 2001.

[9] J. Drake et. al. . in preperation, 2004.

[10] D. Garcia, J. Drake, L. Lin, and V. Kashyap. The Coronae of AB Dor and V471 Tau: Primordial angular momentum vs tidal spin-up. To be submitted to the *Astrophysical Journal*.

[11] N. Grevesse and A. J. Sauval. The solar abundance of iron and the photospheric model. *Astronomy & Astrophysics*, 347:348–354, July 1999.

[12] J. T. Jefferies, F. Q. Orrall, and J. B. Zirker. The Interpretation of Total Line Intensities from Optically Thin Gases. I: A General Method. *Solar Physics*, 22:307–+, 1972.

[13] C. Jordan. The structure and energy balance of solar active regions. *Royal Society of London Philosophical Transactions Series A*, 281:391–404, May 1976.

[14] P. G. Judge, V. Hubeny, and J. C. Brown. Fundamental Limitations of Emission-Line Spectra as Diagnostics of Plasma Temperature and Density Structure. *Astrophysical Journal*, 475:275–+, Jan. 1997.

[15] J. S. Kaastra, R. Mewe, D. A. Liedahl, K. P. Singh, N. E. White, and S. A. Drake. Emission measure analysis methods: the corona of AR Lacertae revisited. *Astronomy & Astrophysics*, 314:547–557, Oct. 1996.

[16] V. Kashyap and J. J. Drake. Markov-Chain Monte Carlo Reconstruction of Emission Measure Distributions: Application to Solar Extreme-Ultraviolet Spectra. *Astrophysical Journal*, 503:450–+, Aug. 1998.

[17] V. Kashyap and J. J. Drake. PINTofALE : Package for the interactive analysis of line emission. *Bulletin of the Astronomical Society of India*, 28:475–476, June 2000.

[18] A. Maggio, J. J. Drake, V. Kashyap, G. Micela, S. Sciortino, G. Peres, F. R. Harnden, and S. S. Murray. AD Leo observed with Chandra LETG: emission measure distribution density, and element abundances of the coronal plasma. In *ASP Conf. Ser. 277: Stellar Coronae in the Chandra and XMM-NEWTON Era*, pages 57–+, 2002.

[19] N. Metropolis, A. Rosenbluth, M. Rosenbluth, A. Teller, and E. Teller. Simulated Annealing. *Journal of Chemical Physics*, 21:1087–1092, 1953.

[20] R. Neal. Probabilistic inference using markov chain monte carlo methods. Technical report, Dept. of Computer Science, University of Toronto, 1993.

[21] S. R. Pottasch. The Lower Solar Corona: Interpretation of the Ultraviolet Spectrum. *Astrophysical Journal*, 137:945–+, Apr. 1963.

[22] W. H. Press, S. A. Teukolsky, W. T. Vetterling, and B. P. Flannery. *Numerical Recipes in C++ The Art of Scientific Computing*. Cambridge University Press, 2002.

[23] J. Schmitt and J.-U. Ness. Coronal abundances from high-resolution X-ray data: The case of Algol. *Astronomy & Astrophysics* accepted.

[24] J. H. M. M. Schmitt, J. J. Drake, R. A. Stern, and B. M. Haisch. The Extreme-Ultraviolet Spectrum of the Nearby K Dwarf epsilon Eridani. *Astrophysical Journal*, 457:882–+, Feb. 1996.

[25] R. K. Smith, N. S. Brickhouse, J. C. Raymond, and D. A. Liedahl. First Results from APEC: The Spectra of Collisionally-Excited Plasmas. *Bulletin of the American Astronomical Society*, 31:735–+, Apr. 1999.

[26] G. L. Withbroe. The analysis of XUV emission lines. *Solar Physics*, 45:301–317, Dec. 1975.